

RESEARCH

Open Access



Pro-fibrotic and apoptotic activities of circARAP1 in myocardial ischemia–reperfusion injury

Xi Li^{1*}, Lei Guo², Jingjing Wang¹ and Xing Yang²

Abstract

Reperfusion modality can cause damage to cardiomyocytes, known as myocardial ischemia–reperfusion injury (MI/RI). Circular RNAs (circRNAs) are fundamental regulators associated with many cardiac diseases, including MI/RI. However, their functional impact on cardiomyocyte fibrosis and apoptosis remains elusive. Therefore, this study aimed to explore possible molecular mechanisms of circARPA1 in animal models and in hypoxia/reoxygenation (H/R)-treated cardiomyocytes. GEO dataset analysis showed that has_circ_0023461 (circARPA1) was differentially expressed in myocardial infarction samples. Real-time quantitative PCR further supported that circARPA1 was expressed at high levels in animal models and in H/R-triggered cardiomyocytes. Then, loss-of-function assays were performed to show that circARAP1 suppression effectively ameliorated cardiomyocyte fibrosis and apoptosis in MI/RI mice. Mechanistic experiments showed that miR-379-5p, KLF9 and Wnt signaling pathways were associated with circARPA1. circARPA1 can sponge miR-379-5p to regulate KLF9 expression, thereby activating the wnt/ β -catenin pathway. Finally, gain-of-function assays revealed that circARAP1 aggravated MI/RI in mice and H/R-induced cardiomyocyte injury by regulating the miR-379-5p/KLF9 axis to activate Wnt/ β -catenin signaling.

Keywords Myocardial ischemia–reperfusion injury, circARPA1, miR-379-5p, KLF9, Wnt pathway

Introduction

Myocardial infarction (MI) causes high disability and mortality in patients with cardiovascular disease worldwide [1]. Timely and complete reperfusion (primary percutaneous coronary intervention and clinical thrombolysis) can decrease mortality from MI [2, 3], reperfusion itself may lead to hypersensitivity irreversible myocardial injury and cardiac dysfunction, namely myocardial ischemia–reperfusion injury (MI/RI) [4]. MI/RI

can lead to a series of adverse effects and damages, such as reinfarction, malignant arrhythmia and heart failure [5]. Currently, the main treatments for MI/RI include ischemic postconditioning, remote ischemic preconditioning, and drug therapy [6]. However, microvascular dysfunction occurs after treatment [7, 8]. Protecting the heart from the deleterious effects of MI/RI remains a therapeutic challenge.

Circular RNAs (circRNAs) are endogenous transcripts that are expressed widely [9] and implicated in multiple cardiovascular diseases [10, 11]. For example, circFoxo3 inhibits autophagy in MI, thereby inhibiting MI/RI [12]. CircHIPK3 offers autophagic and apoptotic properties in MI/RI [13] and circSAM4A can promote hypoxia/reoxygenation (H/R)-induced apoptosis and inflammatory responses [14]. GEO dataset (GSE160717) from the circMine website screened out the differentially expressed

*Correspondence:

Xi Li

lilyspring80@126.com

¹ Department of Cardiology, General Hospital of Ningxia Medical University, No. 804, Shengli South Street, Xingqing District, Yinchuan 750003, Ningxia Hui Autonomous Region, China

² Department of Cardiology, Yan'an University Xianyang Hospital, Xianyang 716099, Shaanxi, China



© The Author(s) 2023. **Open Access** This article is licensed under a Creative Commons Attribution 4.0 International License, which permits use, sharing, adaptation, distribution and reproduction in any medium or format, as long as you give appropriate credit to the original author(s) and the source, provide a link to the Creative Commons licence, and indicate if changes were made. The images or other third party material in this article are included in the article's Creative Commons licence, unless indicated otherwise in a credit line to the material. If material is not included in the article's Creative Commons licence and your intended use is not permitted by statutory regulation or exceeds the permitted use, you will need to obtain permission directly from the copyright holder. To view a copy of this licence, visit <http://creativecommons.org/licenses/by/4.0/>. The Creative Commons Public Domain Dedication waiver (<http://creativecommons.org/publicdomain/zero/1.0/>) applies to the data made available in this article, unless otherwise stated in a credit line to the data.

circRNAs during MI/RI and identified has_circ_0023461 (circARPA1) as the circRNA of interest because of the highest differential expression. However, to date, whether circARPA1 is involved in the development of MI/RI has not been confirmed. Furthermore, the 3'-UTR microRNA (miR)-379-5p contained a putative binding site for circARPA1 and 3-UTR region of KLF9 contained a putative binding site for miR-379-5p. It has been described that KLF9 aggravates ischemic injury in cardiomyocytes by increasing oxidative stress [15]. Given that, this study investigated the underlying molecular mechanisms of circARPA1 in MI/RI and assessed whether circARPA1 could serve as a therapeutic target for MI/RI.

Materials and methods

Cell culture

DMEM (Thermo, USA) consisting of 10% FBS (Gibco, USA) and 1% penicillin/streptomycin was in application to culturing mouse cardiomyocytes HL-1 (ATCC, USA). The in vitro MI/RI model was established on cardiomyocytes cultured for 6 h under conditions of 1% O₂, 5% CO₂ and 94% N₂, and then for 4 h under conditions of 95% air and 5% CO₂.

Cell transfection

siRNA or pcDNA 3.1 overexpression vectors targeting circARPA1 and KLF9, miR-379-5p mimic/inhibitor and their negative controls were designed and provided by GenePharma (Shanghai, China). Following H/R, the above plasmids or oligonucleotides were transfected into HL-1 cells using Lipofectamine 2000 (Invitrogen, USA) and the transfection efficiency was assessed after 48 h. To inhibit the Wnt pathway, cells were pretreated with 10 μM ICG-001 for 0.5 h before transfection.

RNase R test

Trizol method-based extraction of total RNA (4 μg) was performed, followed by RNase R digestion (4 U/μg) for 30 min. The products were analyzed using RT-qPCR.

Actinomycin D test

HL-1 cells were incubated with 2 mg/ml actinomycin D (Sigma-Aldrich, MO, USA), followed by measurements of circRNA or mRNA at different time points (0, 4, 8, 12, 24).

Flow cytometry

Apoptosis detection was performed on HL-1 cells (1 × 10⁶ cells/ml) based on annexin V-fluorescein isothiocyanate/propidium iodide staining kit (Solarbio, China) and data acquisition was completed on a FACS Calibur flow cytometer (BD Biosciences).

ROS detection

ROS production was calculated by 2',7'-dichlorofluorescein diacetate staining (Sigma, USA). Fluorescence intensity was analyzed by flow cytometry.

LDH release and creatine kinase (CK) detection

After I/R modeling, serum samples were separated from the femoral arterial blood of mice. LDH and CK in mouse serum and HL-1 cell supernatant were analyzed by LDH kit (C0017, Beyotime Biotechnology, Shanghai, China) and CK kit (ML-ELISA-0252, R&D Systems).

FISH assay

Subcellular localization of circARPA1 and miR-379-5p was determined using fluorescent probes for Cy3-labeled circARPA1 and Fam-labeled miR-379-5p (Servicebio, Wuhan, China) and FISH kits (Roche, Basel, Switzerland). Cells were first fixed with 4% paraformaldehyde, permeabilized with 0.25% Triton X-100, hybridized with specific labeled probes, and stained with DAPI. Images were taken under a fluorescence microscope (BX53, Olympus).

Nucleocytoplasmic separation

Cytoplasmic and nuclear RNAs were isolated using the PARIS kit (Life Technologies) and conditioned to circARPA1 quantitative analysis.

circRIP and RIP experiments

circRIP assay was performed with BersinBio™ RIP kit (BersinBio, Guangzhou, China) [16] and RIP assay was with EZ-Magna RIP kit (Millipore). HL-1 cells with biotin-NC and biotin-miR-379-5p were lysed in complete RIP lysis buffer and combined with mouse anti-Ago2-conjugated magnetic beads in RIP buffer. Finally, RNA was extracted by the phenol-chloroform method and quantified.

Dual luciferase reporter assay

circARPA1/KLF9 sequences containing wild-type or mutant miR-379-5p binding sites were synthesized and inserted into pmirGLO luciferase vector (GeneCreate, Wuhan, China). HL-1 cells (5 × 10³ cells/well) were placed in a co-transfection system containing miR-379-5p mimic or negative control and vectors based on Lipofectamine 2000 to examine luciferase activity using a dual-luciferase assay system (Promega).

MI/RI modeling

A total of 75 healthy male C57BL/6 mice (6–8 weeks old, 20–30 g) were purchased from SJA Laboratory Animal Co., Ltd. and adaptively housed for 1 week before MI/RI modeling [17]. Briefly, the thoracic cavity was exposed

after intraperitoneal injection of pentobarbital sodium (30 mg/kg), and the left anterior descending artery (LAD) was ligated with silk 6-0. Successful myocardial ischemia, such as myocardial discoloration, decreased pulse, and ST-segment elevation, was observed on the ECG. After 30 min of ischemia, the ligatures were untied to restore blood flow for 120 min. Sham operation excluded LAD ligation. An overexpression vector targeting circARAP1 (oe-circARAP1) and a negative control vector (oe-NC) were injected via tail vein (50 nM) one week before surgery. Wnt signaling inhibitor ICG-001 (5 mg/kg/day, Chembest, China) was injected via tail vein for 5 days after MI/R surgery. After 10 days, the mice were euthanized, 5 mouse hearts in each group were used for TTC staining, and the rest was for routine pathological staining and gene extraction.

Cardiac function

LVDP, LVSP, and ± dp/dtmax were recorded by RM6240B multi-channel physiological signal acquisition and processing system 7 days after MI/RI surgery.

TTC staining

TTC staining was used to assess infarct size. Quickly move the heart to a - 80 °C refrigerator for 20 min. Frozen hearts were cut transversely into 2-mm sections for dyeing with 1% TTC (Sigma-Aldrich). After 4% paraformaldehyde treatment, tissue sections were photographed with a digital camera (Nikon, Tokyo, Japan) and analyzed by Image J software.

HE and Masson staining

Hearts after paraffin-embedding were cut into 4 µm for H&E staining (Beyotime) and Masson staining (Solarbio). After staining, the sections were photographed under a microscope.

TUNEL staining

TUNEL staining was done based on the instructions of in situ cell death detection kit (Roche) and DAPI nuclei staining [18].

IHC staining

After deparaffinization and hydration, sections were blocked with 3% hydrogen peroxide, followed by treatments with 10% normal goat serum (Cat. No. 16210072; Gibco; Thermo Fisher Scientific), primary antibodies α-SMA (A2547, MilliporeSigma), Collagen I (14695-1-AP, Proteintech), Collagen II (15943-1-AP, Proteintech), and HRP-conjugated goat anti-rabbit secondary antibody (1:400; Cat. No. A32731; Invitrogen). After DAB treatment, microscopic images were taken.

RT-qPCR

Total RNA was obtained using the TRIzol RNA isolation system (Life Technologies) and prepared into first-strand cDNA using a reverse transcription system kit (Promega). RT-qPCR was performed in the ABI PRISM 7000 Sequence Detection System (Applied Biosystems, Foster City, CA) in combination with PCR primer sequences (Table 1). Relative gene expression was determined by the 2^{-ΔΔCT} method [19].

Western blot

Cells or heart tissues were lysed in ice-cold RIPA lysis buffer (Solarbio) containing protease inhibitors (Roche) and proteins were separated by 12% SDS-PAGE and transferred to nitrocellulose membranes. Membranes were prepared against α-SMA (A2547, MilliporeSigma), Collagen I (14695-1-AP, Proteintech), Collagen II (15943-1-AP, Proteintech), Wnt1 (ab15251, Abcam), β-catenin (ab32572, Abcam), KLF9 (ab227920, Abcam), cleaved caspase-3 (ab2302, Abcam), Bax (ab32503, Abcam), GAPDH (60004-1-Ig, Proteintech), as well as HRP-conjugated secondary antibody. With Pierce® ECL Western Blot Substrate (Pierce), protein bands were visualized and analyzed by Image J.

Data analysis

Statistical analysis of data with at least three biological replicates was performed using SPSS 21.0. Measurement data were shown as mean ± standard deviation (SD) and evaluated by unpaired t-test for bilateral data or one-way analysis of variance and Tukey’s post hoc test for multiple data. P < 0.05 was considered statistically significant.

Table 1 Primer sequences

Genes	Primer sequences (5’-3’)
circARPA1	Forward: 5’- GTGTTTAGTTGGCGGATGGC-3’ Reverse: 5’- TTGATGACTGGTGTGACGGG-3’
miR-379-5p	Forward: 5’- GCGCGTGTTAGACTATGGAA -3’ Reverse: 5’- GCAGGGTCCGAGGTATTC -3’
KLF9	Forward: 5’- TCTGGAGAGTCCCGATGAGG-3’ Reverse: 5’- GAAAGGGCCGTTTCCCTGTA-3’
Collagen I	Forward: 5’- TTCTCCTGGCAAAGACGGAC-3’ Reverse: 5’- AGTGGCACATCTTGAGGTGCG-3’
Collagen II	Forward: 5’- AGAGGCTTTGATGGACGCAA-3’ Reverse: 5’- CCACCAGGACTGCCGTTATT-3’
U6	Forward: 5’- CTCGCTTCGGCAGCAC-3’ Reverse: 5’- AACGCTTCACGAATTTGCGT-3’
GAPDH	Forward: 5’- CATCAACGGGAAGCCCATC Reverse: 5’- CTCGTGGTTTACACCCATC

Note: circARPA1, circular RNA ARPA1; miR-379-5p, microRNA-379-5p; KLF9, Kruppel-like factor 9; GAPDH, glyceraldehydes-3-phosphate dehydrogenase

Results

CircARAP1 is abnormally overexpressed in MI/RI

To screen out the differential circRNAs during MI/RI, 3 MI samples and 3 normal samples from the GEO dataset (GSE160717) were analyzed through the circMine website. A total of 107 up-regulated and 63 down-regulated circRNAs were found (Supplementary Table 1), of which hsa_circ_0023461 (circARPA1) was identified as the circRNA of interest as having the highest differential expression (log2-fold change = 2.9385) (Fig. 1A–C). Subsequently, gene information of hsacirc0023461 was found on circbase, which is a circular transcript spliced from ARAP1 with a length of 2542 bp, and the gene is located at chr11: 72406762–72423384 (Fig. 1D). Nucleic acid electrophoresis was implemented on the cDNA and gDNA obtained in HL-1 cells and circARAP1 was

amplified by different primers in the cDNA, but not the gDNA (Fig. 1E). RNase R could not digest circARAP1, and actinomycin D could not affect the stability of circARAP1 (Fig. 1F, G), further confirming the ring structure of circARAP1. circARAP1 was abnormally highly expressed in H/R-treated HL-1 cells (Fig. 1H).

Knockdown of circARAP1 improves cardiomyocyte fibrosis and apoptosis

To determine the biological function of circARAP1, circARAP1-targeting siRNA was transfected into HL-1 cells, resulting in the decrease of circARAP1 expression in H/R-injured HL-1 cells (Fig. 2A). In H/R-induced ROS production (Fig. 2B), increased levels of LDH and CK (Fig. 2C), and stimulated apoptosis (Fig. 2D). Also, H/R induced an increase in Collagen I and Collagen II mRNA expression (Fig. 2E). Similar results were obtained by

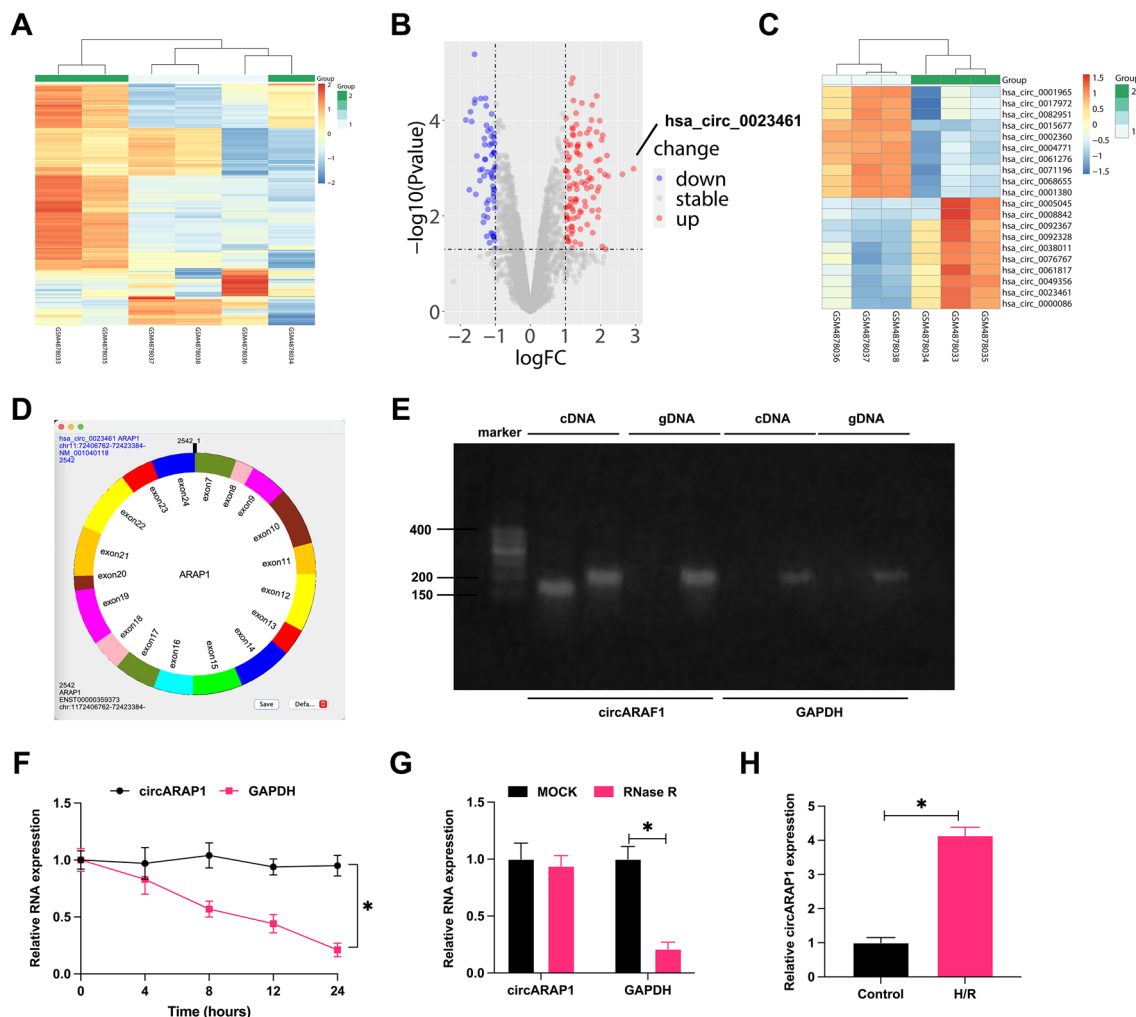


Fig. 1 CircARAP1 is abnormally highly expressed in MI/RI. **A**: Heat map showing the top 250 differential circRNAs; **B**: volcano plot of differential circRNAs; **C**: top ten highly expressed and low expressed circRNAs; **D**: gene information of circARAP1; **E**: circular structure of circARAP1; **F** and **G**: ring structure of circARAP1; **H**: circARAP1 expression in H/R-treated HL-1 cells; data are expressed as mean ± SD (N = 3)

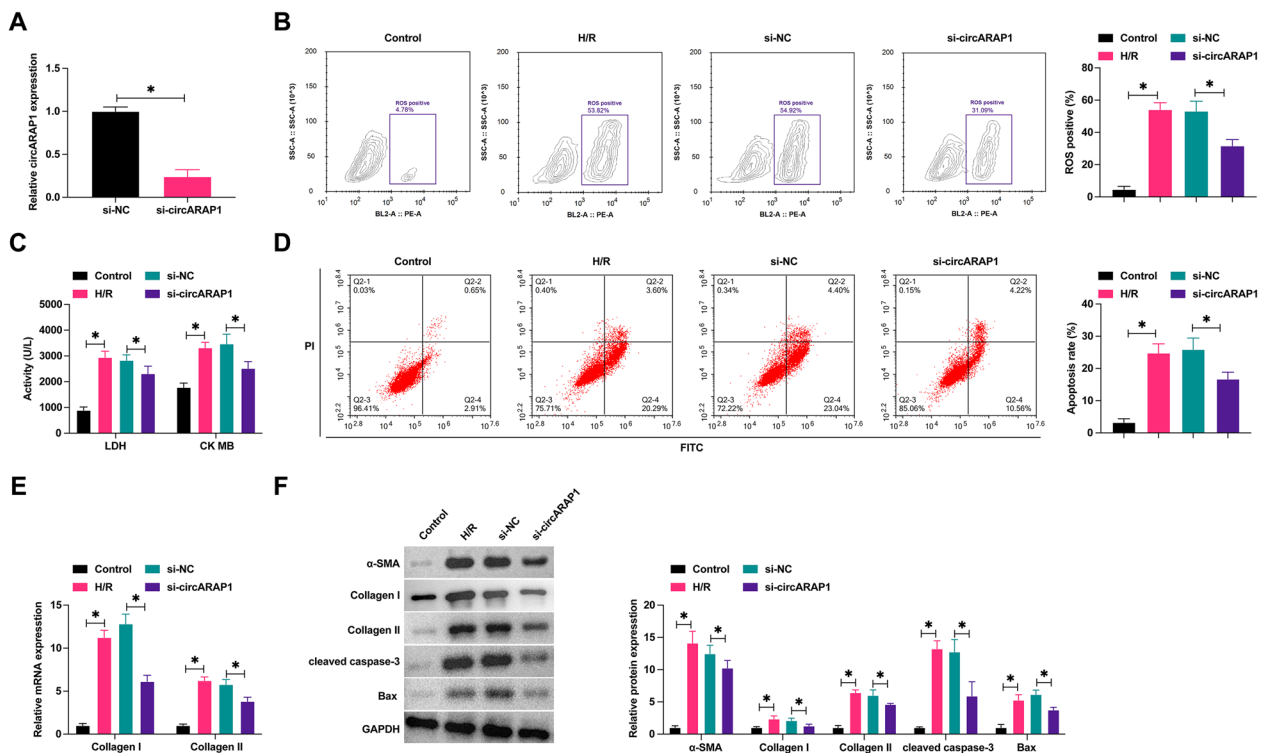


Fig. 2 Knockdown of circARAP1 improves cardiomyocyte fibrosis and apoptosis. siRNA targeting circARAP1 was transfected into H/R-treated HL-1 cells. **A**: circARAP1 expression changes; **B**: ROS production; **C**: LDH and CK levels in HL-1 cells; **D**: apoptosis rate; **E**: Collagen I and Collagen II mRNA in cells; **F**: protein levels of α -SMA, Collagen I, Collagen II, cleaved caspase-3, Bax; data are expressed as mean \pm SD ($N=3$)

Western blot. H/R treatment increased the protein levels of α -SMA, Collagen I, Collagen II, cleaved caspase-3, and Bax (Fig. 2F). The above changes in H/R-treated HL-1 cells were prevented when circARAP1 was knocked down (Fig. 2B–F).

CircARAP1 targets miR-379-5p

CircARAP1 was mainly present in the cytoplasm of HL-1 (Fig. 3A). CircARAP1-adsorbed miRNAs were purified by circRIP experiments, among which 17 miRNAs had potential binding sites with circARAP1 on the

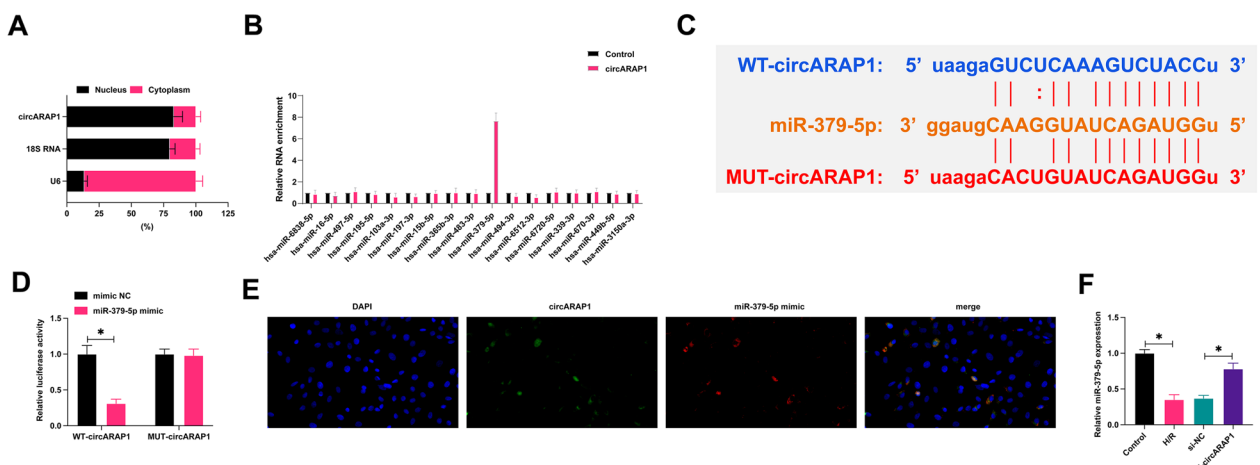


Fig. 3 CircARAP1 targets miR-379-5p. **A**: Subcellular localization of circARAP1; **B**: miRNA adsorbed by circARAP1 purified by circRIP; **C**: potential binding site of circARAP1 and miR-379-5p; **D**: targeting relationship between circARAP1 and miR-379-5p; **E**: co-localization of circARAP1 and miR-379-5p in HL-1 cells; **F**: miR-379-5p expression in cells; data are expressed as mean \pm SD ($N=3$)

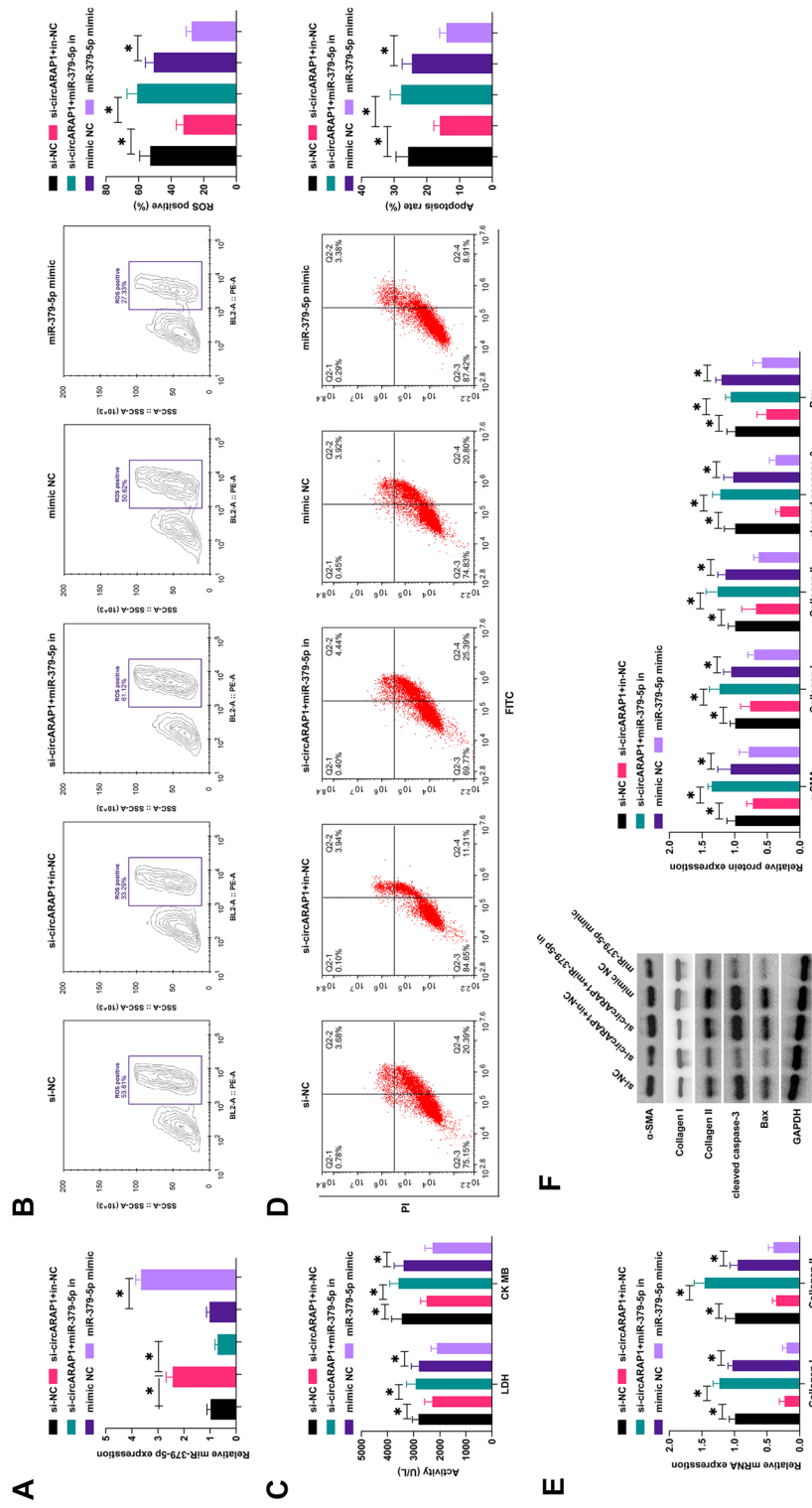


Fig. 4 CircARAP1 by modifying miR-379-5p improves cardiomyocyte fibrosis and apoptosis. si-circARAP1, miR-379-5p mimic/inhibitor was transfected into H/R-treated HL-1 cells. **A:** miR-379-5p expression changes; **B:** ROS production; **C:** LDH and CK levels in HL-1 cells; **D:** cell apoptosis rate; **E:** Collagen I and Collagen II mRNA levels; **F:** protein levels of α-SMA, Collagen I, Collagen II, cleaved caspase-3, Bax; data are expressed as mean ± SD (N=3)

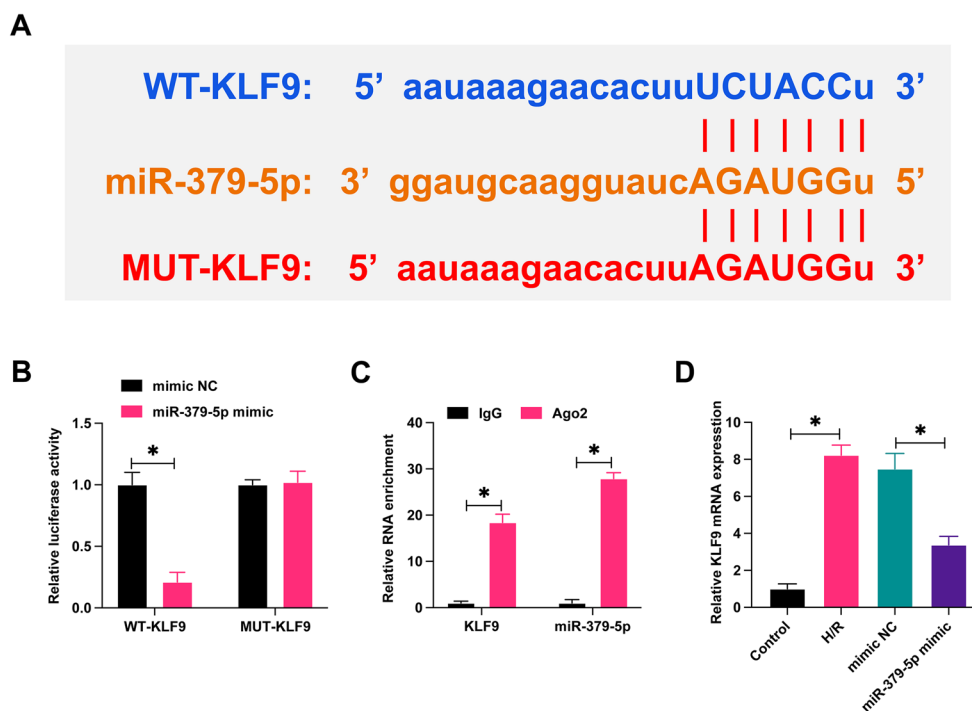


Fig. 5 KLF9 is a target gene of miR-379-5p. **A:** Potential binding sites of KLF9 and miR-379-5p; **B:** targeting relationship of KLF9 and miR-379-5p; **C:** binding relationship of KLF9 and miR-379-5p; **D:** expression changes of KLF9 in H/R-treated HL-1 cells; data are expressed as mean \pm SD (N = 3)

bioinformatics website, and particularly circARAP1 was highly specifically enriched with miR-379-5p (Fig. 3B). Subsequently, based on the predicted binding sites from <https://starbase.sysu.edu.cn> (Fig. 3C), WT-circARAP1 and MUT-circARAP1 luciferase reporters were generated, and co-transfection of MUT-circARAP1 and miR-379-5p mimic did not affect luciferase activity, but luciferase activity decreased after co-transfection of WT-circARAP1 and miR-379-5p mimic (Fig. 3D). FISH analysis presented that circARAP1 and miR-379-5p co-localized in the cytoplasm of HL-1 cells (Fig. 3E). As demonstrated in Fig. 3F, H/R treatment inhibited miR-379-5p expression, but knockdown of circARAP1 restored miR-379-5p expression.

CircARAP1 by modifying miR-379-5p improves cardiomyocyte fibrosis and apoptosis

For confirming the biological function of miR-379-5p in MI/RI and whether it is involved in the process of circARAP1 regulating MI/RI, si-circARAP1, miR-379-5p mimic/inhibitor were transfected into H/ R-treated HL-1 cells. si-ARAP1 or miR-379-5p mimic up-regulated miR-379-5p, while the effect of si-circARAP1 was antagonized by miR-379-5p inhibitor (Fig. 4A). In addition, silencing circARAP1 or inducing miR-379-5p exhibited beneficial effects on ameliorating H/R injury, mainly manifested as decreased ROS production, decreased LDH, CK and

apoptosis rates, and decreased collagen I/II mRNA level, inhibited α -SMA, collagen I/II, cleaved caspase-3 and Bax protein expression, while the effect of knockdown of circARAP1 was blocked when miR-379-5p was inhibited (Fig. 4B–F).

KLF9 is a target gene of miR-379-5p

We queried the potential downstream targets of KLF9 and miR-379-5p from the bioinformatics website <https://starbase.sysu.edu.cn> (Fig. 5A). Subsequently, wild-type and mutant KLF9 luciferase reporter vectors were designed according to potential binding sites and the targeted binding of KLF9 and miR-379-5p was confirmed by dual-luciferase reporter experiments (Fig. 5B). RIP experiments further confirmed that KLF9 and miR-379-5p were significantly enriched (Fig. 5C). By RT-qPCR, it was found that H/R treatment induced an increase in KLF9 expression, whereas overexpression of miR-379-5p prevented this change (Fig. 5D).

CircARAP1 ameliorates cardiomyocyte fibrosis and apoptosis by regulating the miR-379-5p/KLF9 axis

Subsequently, pcDNA 3.1-circARAP1 and si-KLF9 were co-introduced into H/R-treated HL-1 cells. pcDNA 3.1-circARAP1 increased circARAP1 and KLF9 but suppressed miR-379-5p levels, while si-KLF9 decreased KLF9 expression but did not affect circARAP1 and

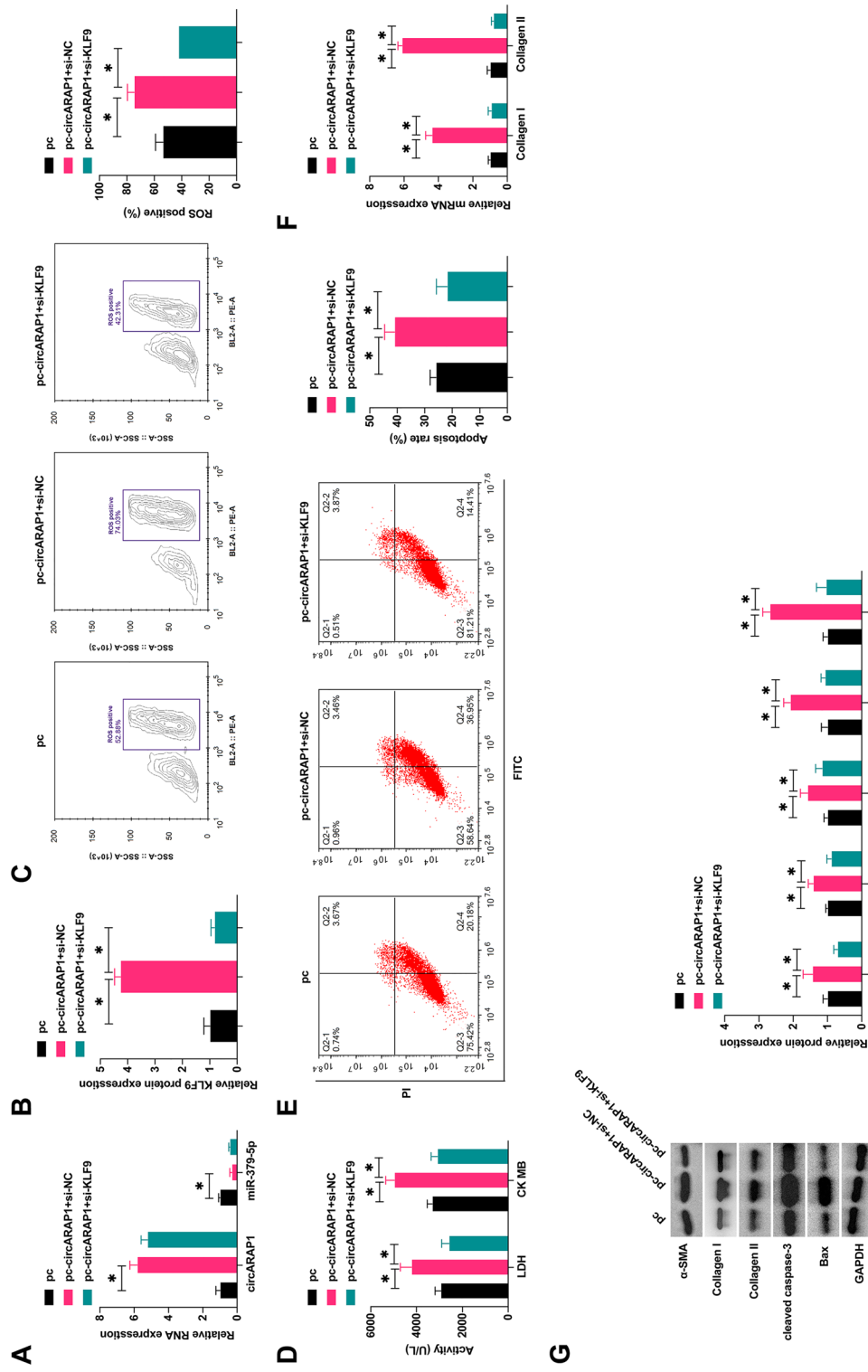


Fig. 6 CircARAP1 improves cardiomyocyte fibrosis and apoptosis by regulating miR-379-5p/KLF9 axis. pcDNA 3.1-circARAP1 and si-KLF9 were co-transfected into H/R-treated HL-1 cells. **A-B:** circARAP1, miR-379-5p, and KLF9 expression changes; **C:** ROS production; **D:** LDH and CK in HL-1 cells; **E:** apoptosis rate; **F:** Collagen I and Collagen II mRNA levels; **G:** protein levels of α -SMA, Collagen I, Collagen II, cleaved caspase-3 and Bax level; data are expressed as mean \pm SD (N = 3)

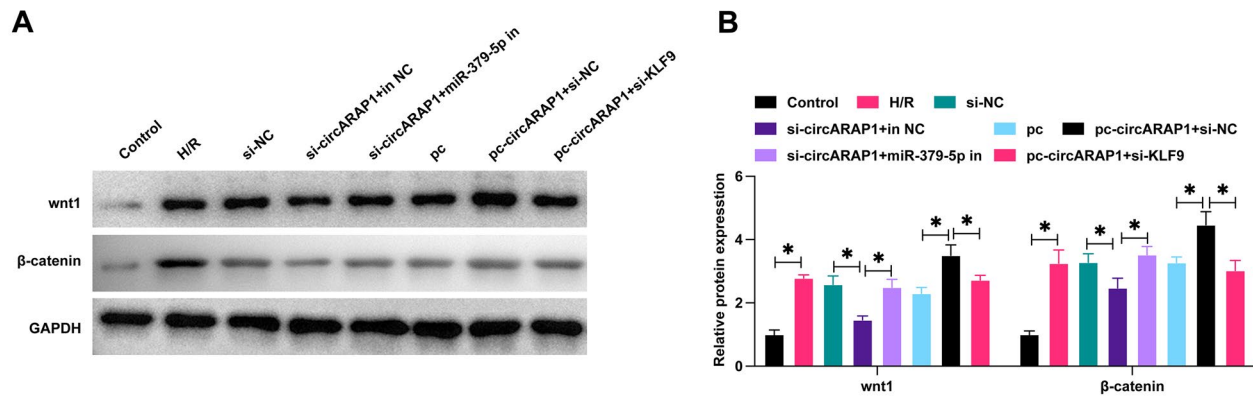


Fig. 7 CircARAP1/miR-379-5p/KLF9 axis regulates Wnt/ β -catenin pathway. **A–B:** Protein expressions of Wnt1 and β -catenin in HL-1 cells; data are expressed as mean \pm SD ($N=3$)

miR-379-5p expression on the basis of pcDNA 3.1-circARAP1 (Fig. 6A, B). circARAP1 induction further aggravated H/R-induced cardiomyocyte fibrosis and apoptosis, and depletion of KLF9 reversed these phenomena (Fig. 6C–G).

CircARAP1/miR-379-5p/KLF9 axis regulates the Wnt/ β -catenin pathway

Wnt/ β -catenin pathway is abnormally activated in I/RI and exacerbates I/RI [20–22]. Therefore, this study speculates that circARAP1 may activate the Wnt/ β -catenin pathway by affecting the miR-379-5p/KLF9 axis. To test this notion, the protein changes in Wnt1 and β -catenin were tested by western blot. As predicted, H/R treatment activated the Wnt/ β -catenin pathway, knockdown or overexpression of circARAP1 prevented and promoted the activation of the Wnt/ β -catenin pathway, respectively, which was mitigated by silencing miR-379-5p and KLF9, respectively (Fig. 7A, B).

Wnt/ β -catenin pathway is critical for circARAP1 to affect H/R injury

Western blot showed that ICG-001 inhibited wnt/ β -catenin signaling in HL-1 cells overexpressing circARAP1 or knocking down KLF9 (Fig. 8A). Functional experiments showed that ICG-001 led to the reduction of ROS production, inhibited LDH, CK, Collagen I/II and decreased apoptosis, while reducing α -SMA, collagen I/II, cleaved caspase-3 and Bax protein expression in HL-1 cells overexpressing circARAP1, and ICG-001 further enhanced the therapeutic effect of KLF9 knockdown on H/R-induced fibrosis and apoptosis (Fig. 8B–F).

CircARAP1 affects MI/RI in mice by regulating miR-379-5p/KLF9 axis-regulated Wnt/ β -catenin pathway

Oe-circARAP1 was injected into MI/RI-injured mice and ICG-001 was utilized to block Wnt/ β -catenin signaling. MI/RI resulted in increased expression of circARAP1, KLF9, wnt1 and β -catenin and decreased expression of miR-379-5p, while oe-circARAP1 further enhanced the effect of H/R on these genes, but ICG-001 attenuated the effect of oe-circARAP1 (Fig. 9A, B). Detection of cardiac function showed that MI/RI mice had higher LVDP, but lower LVSP, \pm dp/dtmax, and oe-circARAP1 enhanced this change, but blocking Wnt/ β -catenin signaling attenuated this effect of oe-circARAP1 (Fig. 9C). Tissue staining showed that MI/RI mice exhibited larger myocardial infarct size, more severe myocardial tissue damage, more collagen deposition and higher apoptosis rate, oe-circARAP1 aggravated these pathological changes, but blocking the Wnt/ β -catenin pathway attenuated the effect of oe-circARAP1 (Fig. 9D–G). Also, LDH, CK, α -SMA, collagen I/II, cleaved caspase-3 and Bax in MI/RI mice were higher, and oe-circARAP1 further up-regulated the levels of these factors, but disruption of Wnt/ β -catenin pathway attenuated the effect of oe-circARAP1 (Fig. 9H–K).

Discussion

CircRNA is a novel regulatory RNA involved in multiple pathological cardiac progression [23]. Here, circARAP1 was identified as the circRNA of interest. However, to date, the role of circARAP1 in MI-induced myocardial injury remains obscure. In the current study, we identified circARAP1 as a circular RNA and found that

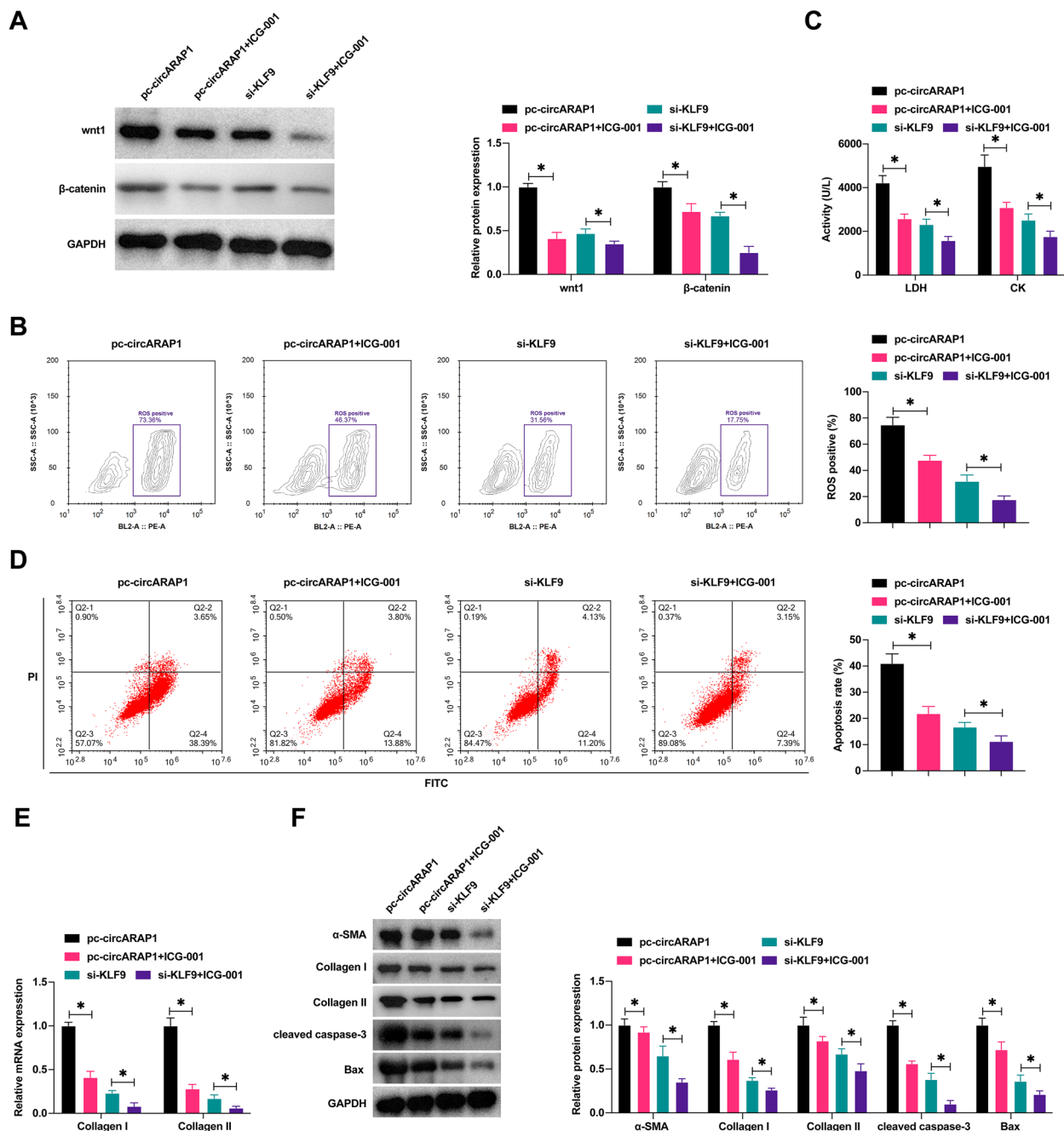


Fig. 8 Wnt/β-catenin pathway is critical for circARAP1 to affect H/R injury. ICG-001 blocked the wnt/β-catenin pathway in HL-1 cells overexpressing circARAP1 or knocking down KLF9. **A**: Protein expressions of Wnt1 and β-catenin; **B**: ROS production; **C**: LDH and CK in HL-1 cells; **D**: apoptosis rate; **E**: Collagen I and Collagen II mRNA levels; **F**: protein levels of α-SMA, Collagen I, Collagen II, cleaved caspase-3, Bax; data are expressed as mean ± SD (N = 3)

circARAP1 was abnormally highly expressed in MI/R-injured mice and H/R-induced cardiomyocytes. Furthermore, we identified novel functions and mechanisms of circARAP1 in regulating myocardial fibrosis and apoptosis in MI/RI.

Myocardial apoptosis and fibrosis are one of the main mechanisms in the progression of MI/RI [24, 25]. The earliest and predominant form of infarcted cardiomyocyte death is apoptosis [24]. Cardiac fibrosis is caused by excessive deposition of extracellular matrix and

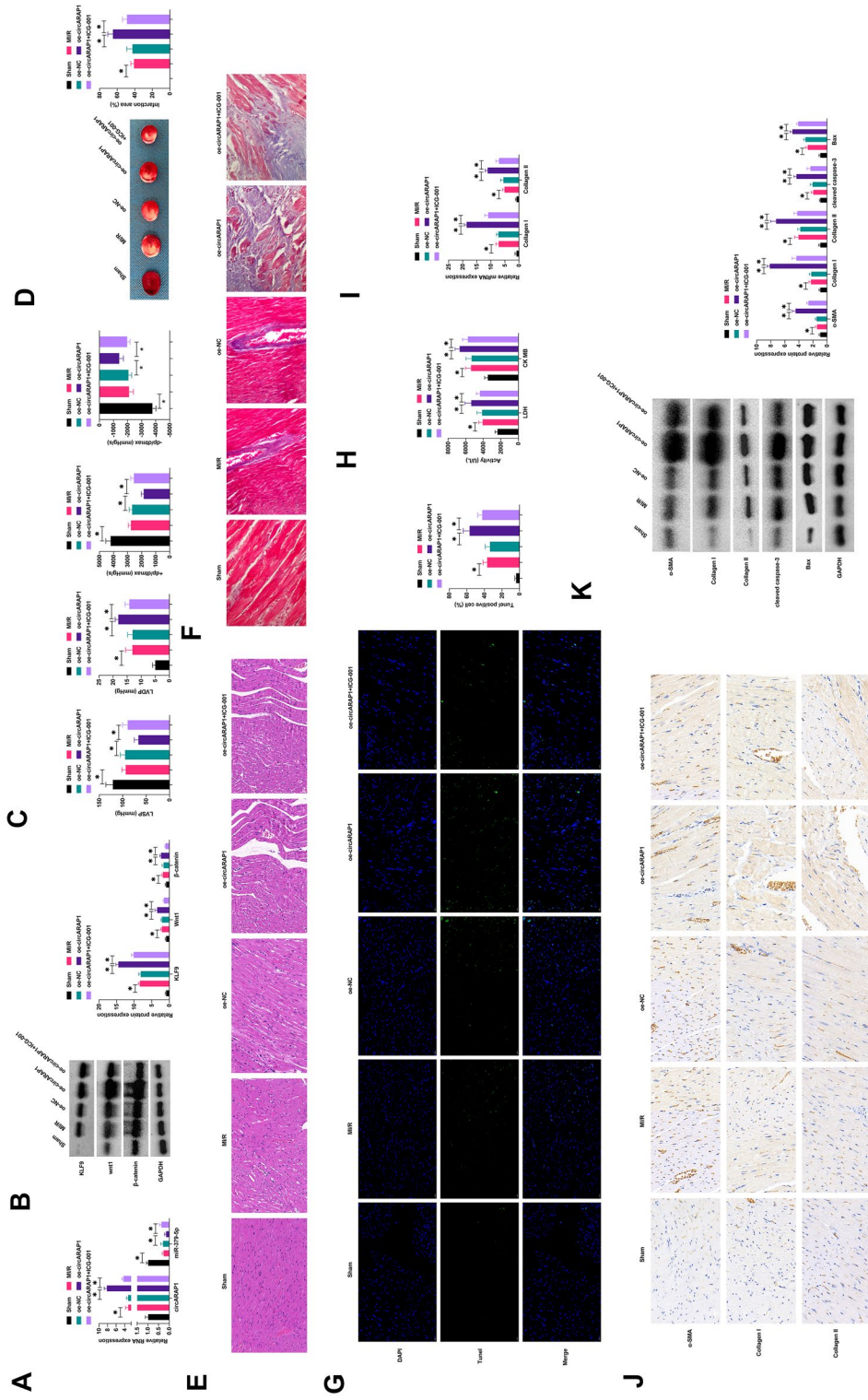


Fig. 9 CircARAP1 affects MI/R1 in mice by regulating miR-379-5p/KLF9 axis and activating Wnt/ β -catenin signaling. Oe-circARAP1 was injected into MI/R-injured mice, and ICG-001 was used to block Wnt/ β -catenin signaling. **A:** circARAP1 and miR-379-5p mRNA levels; **B:** protein expression of KLF9, wnt1 and β -catenin; **C:** mouse cardiac function index; **D:** representative graph of cardiac TTC staining; **E:** representative IMAGES of myocardial tissue HE staining; **F:** protein expression of Masson staining in myocardial tissue; **G:** representative graph of TUNEL staining in myocardial tissue; **H:** serum LDH and CK levels in mice; **I:** Collagen I/II levels in mouse myocardial tissue; **J:** IHC staining of α -SMA, collagen I/II in myocardial tissue; **K:** protein level of α -SMA, Collagen I, Collagen II, cleaved caspase-3, Bax in myocardial tissue; data are expressed as mean \pm SD (D, n = 5; **A-C-E-K**, n = 10)

activation of myofibroblasts in damaged areas, leading to scarring and permanent impairment of cardiac function [26]. Therefore, elucidating the underlying mechanisms of myocardial fibrosis and apoptosis and identifying new strategies are crucial for the treatment of MI/RI. Oxidative damage in the myocardium due to the overproduction of ROS exacerbates cardiomyocyte apoptosis and myocardial fibrosis [27, 28]. Here, it was found that H/R treatment promoted ROS production, increased levels of LDH and CK, protected cardiomyocytes by inhibiting apoptosis and fibrosis, as demonstrated by H/R leading to increased cardiomyocyte apoptosis rates and increased expression of fibrotic and apoptotic indicators, while knockdown of circARAP1 reversed these phenomena.

Cytoplasmic circRNAs competitively bind miRNAs, thereby exerting effects on gene regulation [29]. circARAP1 was mainly present in the cytoplasm of HL-1, suggesting that circARAP1 mainly acts as a ceRNA for downstream miRNAs to play a post-transcriptional regulation role on downstream gene expression. miR-379-5p highly specifically enriched with circARAP1 was screened. Most studies on miR-379-5p have focused on cancer research [30–32], and it has been implicated to exhibit neuroprotective effects against ischemic stroke and reduce neuronal autophagy [33]. Furthermore, in the treatment of atherosclerosis, miR-379-5p is involved in growth, migration and invasion of vascular smooth muscle cells [34]. This study performed a functional rescue experiment to reveal that miR-379-5p was beneficial to ameliorate cardiomyocyte fibrosis and apoptosis.

KLF transcription factor family consists of 17 members that can regulate various biological processes, and alterations in their function have been implicated in the pathobiology of many human diseases, including cardiovascular diseases [35]. KLF9, also known as BTE-B1 [36], has recently been demonstrated to aggravate ischemic injury in cardiomyocytes by increasing oxidative stress [15]. Interestingly, this study found that KLF9, a downstream target gene of miR-379-5p, was up-regulated in H/R-induced HL-1 cells. As expected, data analysis supported that circARAP1 ameliorates H/R-induced cardiomyocyte fibrosis and apoptosis by regulating the miR-379-5p/KLF9 axis.

Wnt/ β -catenin pathway plays a key role in cell growth, differentiation, migration, polarity and death [37]. Recently, the wnt/ β -catenin pathway has been shown to be abnormally activated in I/RI [20–22]. The present study exhibited that circARAP1 activates the Wnt/ β -catenin pathway by regulating the miR-379-5p/KLF9 axis to affect cardiomyocyte H/R injury and MI/RI in mice.

Although the effect of circARAP1 on MI/RI was assessed, the clinical significance of circARAP1 in MI/

RI should be confirmed in future studies. Also, impacts of circARAP1 on other kinds of cardiomyocytes need to be clarified, such as H9c2 and AC16 cells. Finally, the molecular mechanisms responsible for the production and upregulation of circARAP1 require further in-depth study.

Conclusion

CircARAP1 aggravates myocardial ischemia-induced fibrosis and apoptosis by regulating the miR-379-5p/KLF9 axis to activate the Wnt/ β -catenin pathway, and circARAP1 may be a promising therapeutic mechanism for MI/RI.

Acknowledgements

Not applicable.

Author contributions

Conceptualization, XL; methodology, XL and LG; formal analysis, LG and JW; investigation, JW and XY; data curation, LG and XY; writing—original draft preparation, XL; writing—review and editing, XL; project administration, XL. All authors have read and agreed to the published version of the manuscript. All authors read and approved the final manuscript.

Funding

2021 Ningxia Natural Science Foundation (No.2021AAC03324).

Availability of data and materials

Data are available from the corresponding author on request.

Declarations

Ethics approval and consent to participate

All animal experiments complied with the ARRIVE guidelines and performed in accordance with the National Institutes of Health Guide for the Care and Use of Laboratory Animals. The experiments were approved by the Institutional Animal Care and Use Committee of General Hospital of Ningxia Medical University. Written informed consent was obtained from each subject.

Consent for publication

All authors approved the final manuscript and agreed to publish.

Competing interests

The authors have no conflicts of interest to declare.

Received: 7 January 2023 Accepted: 8 January 2023

Published online: 20 February 2023

References

- Mao S, et al. Overexpression of PLK1 relieved the myocardial ischemia-reperfusion injury of rats through inducing the mitophagy and regulating the p-AMPK/FUNDC1 axis. *Bioengineered*. 2021;12(1):2676–87.
- Mehta S, et al. Complete revascularization with multivessel pci for myocardial infarction. *N Engl J Med*. 2019;381(15):1411–21.
- Gill S, et al. Early reperfusion assessment and repeated thrombolysis in acute myocardial infarction estimated by repeated standard electrocardiography a randomised, double-blind, placebo-controlled pilot study. *Cardiology*. 2000;94(1):58–65.
- Huang F, et al. Non-coding RNAs modulate autophagy in myocardial ischemia-reperfusion injury: a systematic review. *J Cardiothorac Surg*. 2021;16(1):140.

5. Benjamin E, et al. Heart disease and stroke statistics-2018 update: a report from the American Heart Association. *Circulation*. 2018;137(12):e67–492.
6. Dalen J, et al. The epidemic of the 20 (th) century: coronary heart disease. *Am J Med*. 2014;127(9):807–12.
7. Mauer mann E, Puelacher C, Lurati Buse G. Myocardial injury after non-cardiac surgery: an underappreciated problem and current challenges. *Current Opin Anaesthesiol*. 2016;29(3):403–12.
8. Heusch G, Gersh B. The pathophysiology of acute myocardial infarction and strategies of protection beyond reperfusion: a continual challenge. *Eur Heart J*. 2017;38(11):774–84.
9. Kristensen L, et al. The biogenesis, biology and characterization of circular RNAs. *Nat Rev Genet*. 2019;20(11):675–91.
10. Altesha M, et al. Circular RNA in cardiovascular disease. *J Cell Physiol*. 2019;234(5):5588–600.
11. Huang C, et al. Cardioprotective effect of circ_SMG6 knockdown against myocardial ischemia/reperfusion injury correlates with miR-138-5p-mediated EGR1/TLR4/TRIF inactivation. *Oxid Med Cell Longev*. 2022;2022:1927260.
12. Sun G, et al. Circular RNA Foxo3 relieves myocardial ischemia/reperfusion injury by suppressing autophagy via inhibiting HMGB1 by repressing KAT7 in myocardial infarction. *J Inflamm Res*. 2021;14:6397–407.
13. Qiu Z, et al. CircHIPK3 regulates the autophagy and apoptosis of hypoxia/reoxygenation-stimulated cardiomyocytes via the miR-20b-5p/ATG7 axis. *Cell Death Discov*. 2021;7(1):64.
14. Hu X, et al. CircSAM4A aggravates H/R-induced cardiomyocyte apoptosis and inflammatory response by sponging miR-138-5p. *J Cell Mol Med*. 2022;26(6):1776–84.
15. Yan Q, et al. KLF9 aggravates ischemic injury in cardiomyocytes through augmenting oxidative stress. *Life Sci*. 2019;233: 116641.
16. Zhou M, et al. The circular RNA circZFR phosphorylates Rb promoting cervical cancer progression by regulating the SSBP1/CDK2/cyclin E1 complex. *J Exp Clin Cancer Res*. 2021;40(1):48.
17. Song Y, et al. The circular RNA TLK1 exacerbates myocardial ischemia/reperfusion injury via targeting miR-214/RIPK1 through TNF signaling pathway. *Free Radical Biol Med*. 2020;155:69–80.
18. Liu X, et al. Mild therapeutic hypothermia protects the brain from ischemia/reperfusion injury through upregulation of iASPP. *Aging Dis*. 2018;9(3):401–11.
19. Xiao L, et al. Sustained activation of Wnt/ β -catenin signaling drives AKI to CKD progression. *J Am Soc Nephrol*. 2016;27(6):1727–40.
20. Li N, et al. MeCP2 attenuates cardiomyocyte hypoxia/reperfusion-induced injury via regulation of the SFRP4/Wnt/ β -catenin axis. *Biomarkers Biochem Indic Exposure, Response Susceptibility Chem*. 2021;26(4):363–70.
21. Dong Q, et al. Wnt/ β -catenin signaling pathway promotes renal ischemia-reperfusion injury through inducing oxidative stress and inflammation response. *J Recept Signal Transduct Res*. 2021;41(1):15–8.
22. Pan W, Xu Z. Triptolide mediates Wnt/ β -catenin signalling pathway to reduce cerebral ischemia-reperfusion injury in rats. *Folia Neuropathol*. 2020;58(4):324–33.
23. Huang C, et al. Circ_ZNF512-Mediated miR-181d-5p inhibition limits cardiomyocyte autophagy and promotes myocardial ischemia/reperfusion injury through an EGR1/mTORC1/TFEB-based mechanism. *J Med Chem*. 2022;65(3):1808–21.
24. Chen L, et al. Targeting MIAT reduces apoptosis of cardiomyocytes after ischemia/reperfusion injury. *Bioengineered*. 2019;10(1):121–32.
25. Lal H, et al. Cardiac fibroblast glycogen synthase kinase-3 β regulates ventricular remodeling and dysfunction in ischemic heart. *Circulation*. 2014;130(5):419–30.
26. Lee T, et al. Conditioned medium from adipose-derived stem cells attenuates ischemia/reperfusion-induced cardiac injury through the microRNA-221/222/PUMA/ETS-1 pathway. *Theranostics*. 2021;11(7):3131–49.
27. Li M, et al. Changes in matrix metalloproteinase-9 levels during progression of atrial fibrillation. *J Int Med Res*. 2014;42(1):224–30.
28. Xue Y, et al. via8-Gingerol ameliorates myocardial fibrosis by attenuating reactive oxygen species, apoptosis, and autophagy the PI3K/Akt/mTOR signaling pathway. *Front Pharmacol*. 2021;12: 711701.
29. Su Y, et al. Circular RNA Foxo3 in cardiac ischemia-reperfusion injury in heart transplantation: a new regulator and target. *Am J Transpl Off J Am Soc Transpl Am Soc Transpl Surg*. 2021;21(9):2992–3004.
30. Chen J, et al. Effects of microRNA-379-5p on proliferation, migration and invasion of hepatocellular carcinoma cell line. *Zhonghua Yi Xue Za Zhi*. 2016;96(18):1450–3.
31. Wu D, et al. MicroRNA-379-5p plays a tumor-suppressive role in human bladder cancer growth and metastasis by directly targeting MDM2. *Oncol Rep*. 2017;37(6):3502–8.
32. Yang B, et al. MiR-379-5p targets microsomal glutathione transferase 1 (MGST1) to regulate human glioma in cell proliferation, migration and invasion and epithelial-mesenchymal transition (EMT). *Biochem Biophys Res Commun*. 2021;568:8–14.
33. Mo Y, et al. MicroRNA-379-5p targets MAP3K2 to reduce autophagy and alleviate neuronal injury following cerebral ischemia via the JNK/c-Jun signaling pathway. *Kaohsiung J Med Sci*. 2022;38(3):230–43.
34. Zheng X, et al. Circ_0002984 enhances growth, invasion, and migration in PDGF-bb-induced vascular smooth muscle cells through miR-379-5p/FRS2 Axis. *J Cardiovasc Pharmacol*. 2021;78(6):875–84.
35. McConnell B, Yang V. Mammalian Krüppel-like factors in health and diseases. *Physiol Rev*. 2010;90(4):1337–81.
36. Ma L, et al. in vitro MicroRNA-142-3p suppresses endometriosis by regulating KLF9-mediated autophagy and. *RNA Biol*. 2019;16(12):1733–48.
37. El-Sahli S, et al. Wnt signaling in cancer metabolism and immunity. *Cancers*. 2019;11(7):904.

Publisher's Note

Springer Nature remains neutral with regard to jurisdictional claims in published maps and institutional affiliations.

Ready to submit your research? Choose BMC and benefit from:

- fast, convenient online submission
- thorough peer review by experienced researchers in your field
- rapid publication on acceptance
- support for research data, including large and complex data types
- gold Open Access which fosters wider collaboration and increased citations
- maximum visibility for your research: over 100M website views per year

At BMC, research is always in progress.

Learn more biomedcentral.com/submissions

